

Microscopic phase diagram of LaFeAsO single crystals under pressurePhilipp Materne,^{1,*} Wenli Bi,^{2,1} Jiyong Zhao,¹ Michael Y. Hu,¹ Rhea Kappenberger,^{3,4} Sabine Wurmehl,^{3,4} Saicharan Aswartham,³ Bernd Büchner,^{3,4} and E. Ercan Alp¹¹Argonne National Laboratory, Lemont, Illinois 60439, USA²Department of Geology, University of Illinois at Urbana-Champaign, Urbana, Illinois 61801, USA³Leibniz Institute for Solid State and Materials Research (IFW), D-01069 Dresden, Germany⁴Institute of Solid State and Materials Physics, TU Dresden, D-01069 Dresden, Germany

(Received 20 August 2018; revised manuscript received 31 October 2018; published 26 November 2018)

We investigated a LaFeAsO single crystal by means of synchrotron Mössbauer spectroscopy under pressure up to 7.5 GPa and down to 13 K and provide a microscopic phase diagram. We found a continuous suppression of the magnetic hyperfine field with increasing pressure, and it completely vanishes at ~ 7.5 GPa, which is in contrast to the behavior in polycrystalline samples where the magnetic order vanishes at ~ 20 GPa. The different behaviors of the polycrystalline samples might be due to As vacancies. Our results are in qualitative agreement with density functional theory calculations where a reduction of the magnetic moment with increasing pressure was found. We found that among different samples the magnetic phase-transition temperature as well as the low-temperature magnetic hyperfine field decrease with increasing unit-cell volume.

DOI: [10.1103/PhysRevB.98.174510](https://doi.org/10.1103/PhysRevB.98.174510)**I. INTRODUCTION**

LaFeAsO as a member of the 1111 family is one of the most studied compounds of the iron-based superconductors. It offers high superconducting transition temperatures in the case of F substitution [1,2] or multiple antiferromagnetic phases in the case of P substitution [3]. Additionally LaFeAsO is theoretically approachable without the additional complication due to $3d-4f$ interaction in other rare-earth 1111 compounds, such as CeFeAsO, SmFeAsO, or PrFeAsO [4–6]. In this paper, we mainly focused on the pressure-dependent phase diagram on LaFeAsO single crystals.

Upon cooling, LaFeAsO exhibits a structural phase transition from $P4/nmm$ to $Cmma$ at 145 K and shows spin-density wave order below 127 K [7]. Measurements on polycrystalline samples have shown that the magnetic order is suppressed with increasing pressure and fully vanishes for pressures of ~ 20 GPa [8,9]. On the other hand, single-crystal resistivity measurements by McElroy *et al.* have shown that the suppression of the magnetic order with increasing pressure is much stronger than in polycrystalline samples [10]. They found a nearly linear reduction of the magnetic ordering temperature to around 60 K at 6 GPa and extrapolated that the critical pressure for a full suppression of the magnetic order is 8–10 GPa. Following up on their work we investigated the microscopic magnetic phase diagram of LaFeAsO under pressure by means of synchrotron Mössbauer spectroscopy (SMS). We found that LaFeAsO single crystals behave differently from polycrystalline samples and that the magnetic order is already vanished at ~ 7.5 GPa.

II. EXPERIMENTAL DETAILS

A LaFeAsO single crystal was investigated by means of SMS, also known as nuclear resonant forward scattering at the beamline 3ID-B of the Advanced Photon Source (APS), Argonne National Laboratory, USA. The single-crystal growth including full characterization is described in detail elsewhere [7]. The SMS experiments were performed in the hybrid filling operation mode of the APS in linear polarization of the beam and with a bunch separation time of 1594 ns. This large time window allows for a high-precision measurement of weak hyperfine interactions. The single crystals were enriched with 15% ^{57}Fe to ensure a sufficient count rate. SMS spectra were recorded between 13 and 125 K and at applied pressures between 0.5 and 7.5 GPa using a special He-flow cryostat and a miniature diamond-anvil cell [11,12]. Diamond anvils with 800 μm culet size were used. A Re gasket was preindented to 140 μm and a hole of 400 μm diameter was electrical discharge machining drilled to act as a sample chamber. Daphne oil 7575 was used as the pressure-transmitting medium ensuring quasihydrostaticity. The pressure was measured *in situ* using an online ruby system and changed at 100 K by a gas membrane system. The uncertainty in the pressure determination is 0.1 GPa. The beam size was $15 \times 20 \mu\text{m}^2$ full width at half maximum. CONUSS was used to analyze the SMS data [13]. For a detailed introduction into SMS, the interested reader is referred to the reviews by Sturhahn *et al.* [14] and Sturhahn [15].

III. RESULTS AND DISCUSSION

Synchrotron Mössbauer spectra for representative pressures and temperatures are shown in Fig. 1. No quantum beats were observed in the paramagnetic temperature regime in the investigated pressure region. However, the paramagnetic

*pmaterne@anl.gov

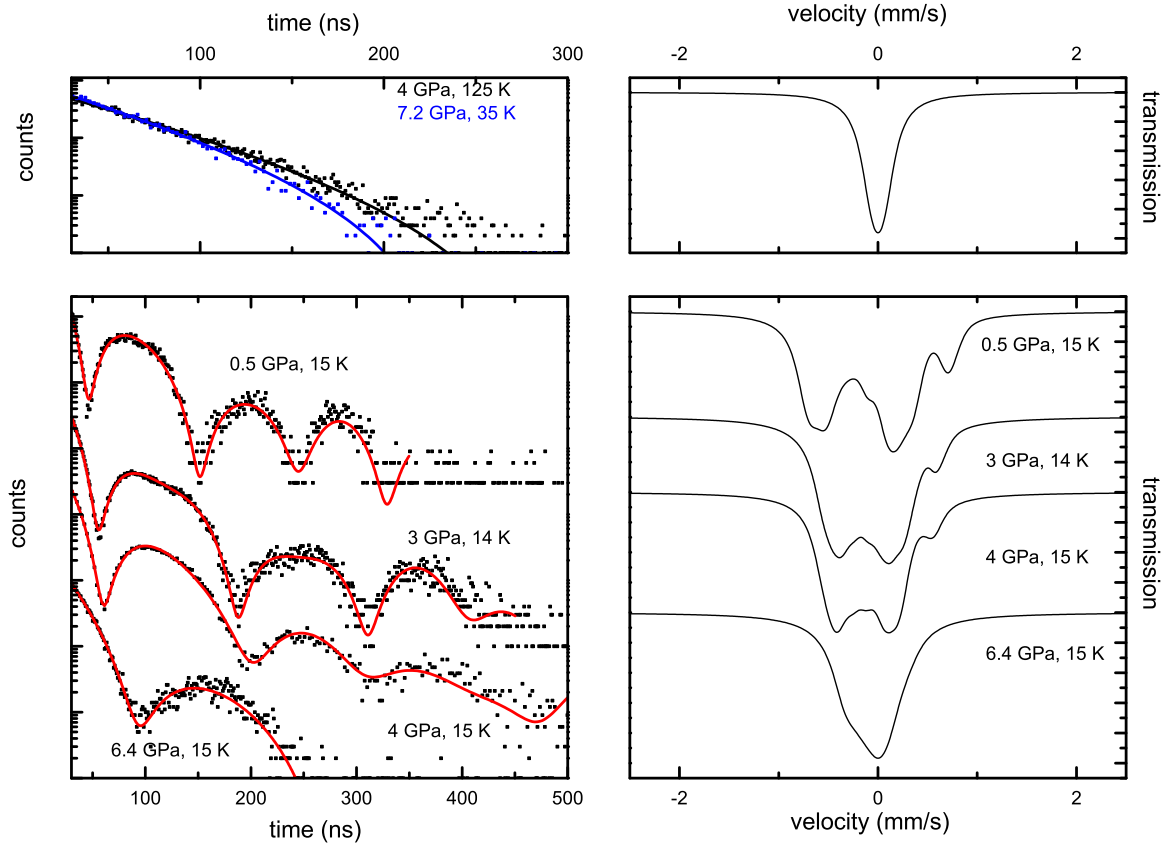


FIG. 1. Synchrotron Mössbauer spectroscopy spectra for representative pressures and temperatures (left column) and the calculated corresponding spectra in the energy domain (right column). Lines in the left column are fits to the data. Top row: spectra in the paramagnetic temperature regime. The absence of any quantum beats indicates no electric-field gradient and no magnetic hyperfine field at the Fe nucleus. Bottom row: the quantum beating patterns show the magnetic order in the sample. The increase in the quantum beat period indicates the reduction of the magnetic hyperfine field with increasing pressure. The energy spectra in the right column were calculated using the hyperfine parameters of the corresponding time spectra. For the isomer shift determination a measurement with a reference sample would have been necessary. The isomer shift in the energy spectra was set to zero for the sake of clarity only as no value for the isomer shift was determined.

spectra in Fig. 1 show a downturn at higher times. In a SMS experiment the time evolution of the coherent decay is determined by two effects: (i) the quantum beats caused by hyperfine fields and (ii) the dynamical beats. The latter is a function of the so-called effective thickness $t_a = f_{ML} n_a \sigma_0 d$ where f_{ML} denotes the Mössbauer-Lamb factor, n_a denotes the ^{57}Fe concentration, σ_0 denotes the nuclear resonant cross section, and d denotes the physical thickness. The latter three are constant. The Mössbauer-Lamb factor is only known for the compound at ambient conditions and 5.5 GPa [16]. We fitted t_a to account for the change in the Mössbauer-Lamb factor as a function of temperature. The dynamical beats are described by Bessel functions within dynamical theory, whereas the quantum beat manifests itself as a periodic function [17]. Therefore both components could be disentangled. The downturn of the time spectra at higher times in the paramagnetic phase is caused by the dynamical beat. However, data were only collected up to ~ 350 – 400 ns, and a tiny quadrupole splitting cannot be ruled out. The upper limit for the quadrupole splitting is ~ 0.04 mm/s which corresponds to an electric-field gradient at the Fe nucleus of close to zero. Therefore we conclude that the FeAs tetrahedra is uniformly compressed with increasing

pressure. Additionally, this indicates quasihydrostatic pressure conditions. In the magnetic phase the quadrupole splitting is ~ 0.34 mm/s at 0.5 GPa and decreases to ~ 0.3 and ~ 0.2 mm/s at 4 and 6.4 GPa, respectively. At ambient pressure in polycrystalline samples quadrupole splittings of 0.12 to 0.3 mm/s were reported which are in fair agreement with our results [9,18,19]. Studies in CeFeAsO and FeSe indicate that the increase in the quadrupole splitting is a result of the magnetic ordering and that the influence of the orthorhombic distortion is negligible [20,21].

In the magnetically ordered phase, the SMS spectra quantum beats arise from the nuclear Zeeman splitting. With increasing pressure the quantum beat period increases indicating a reduction of the magnetic hyperfine field. The magnetic phase-transition region was modeled using a paramagnetic and magnetically ordered signal fraction indicating values of the magnetic volume fraction (MVF) between zero and one. From the temperature dependence of the MVF, which is shown in Fig. 2, two characteristic temperatures for the magnetic phase-transition T_N^{onset} and $T_N^{100\%}$ can be extracted. T_N^{onset} describes the highest temperature with a nonzero MVF, whereas $T_N^{100\%}$ is the highest temperature with 100% MVF

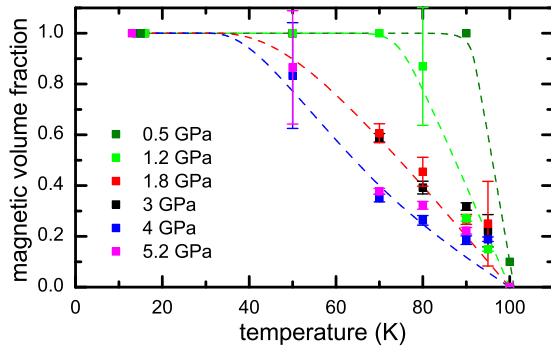


FIG. 2. Magnetic volume fraction as a function of temperature for various pressures. The dashed lines are guides to the eye only. A broadening of the magnetic phase-transition area up to 5.2 GPa was observed.

and both are shown in Fig. 3. T_N^{onset} remains constant within error bars at ~ 95 K up to 5.2 GPa and is vanished at 7.5 GPa.

In contrast $T_N^{100\%}$ is reduced with increasing pressure to 40(15) K at 5.2 GPa. Therefore, the magnetic phase-transition region $\Delta T = T_N^{\text{onset}} - T_N^{100\%}$ increases from 0 to ~ 60 K for 0 and 5.2 GPa, respectively. This increase in ΔT was also seen in muon spin-relaxation experiments under pressure [22]. An increase in ΔT is commonly attributed to a spatial distribution of T_N [20,23–25]. A possible cause could be an increased strain from a lattice misfit with increasing pressure [26]. For 6.4 and 7.2 GPa an extraction of the MVF was not possible due to small magnetic hyperfine fields. Thus the MVF was set to one during the analysis of those pressures in the magnetic phase-transition region. However, this does not influence the analysis of the low-temperature data.

The magnetic hyperfine field as a function of temperature for representative pressure values is shown in Fig. 4. A reduction of the magnetic hyperfine field with increasing pressure was observed.

The low-temperature magnetic hyperfine field as a function of pressure is shown in Fig. 5. The low-temperature magnetic

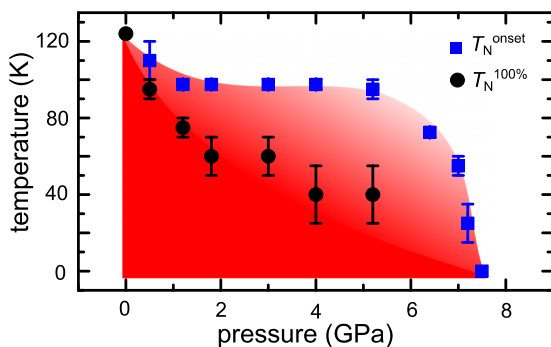


FIG. 3. Characteristic temperatures of the magnetic phase transition: T_N^{onset} (black square) and $T_N^{100\%}$ (red circle) for the investigated pressure regime. T_N^{onset} describes the highest temperature with a nonzero magnetic volume fraction, and $T_N^{100\%}$ is the highest temperature with 100% MVF. For 6.4 and 7.2 GPa, no magnetic volume fraction was extractable from the data, and therefore only T_N^{onset} is shown. The lines are a guide to the eye only. The data point at ambient pressure is taken from Ref. [7].

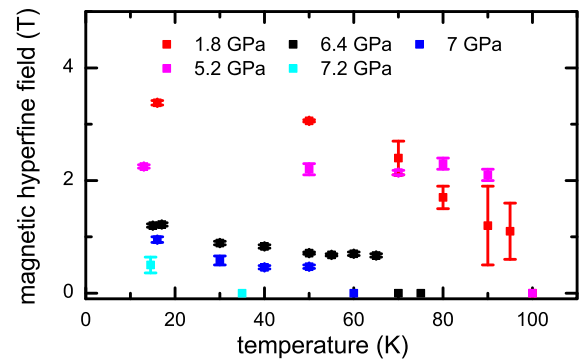


FIG. 4. Magnetic hyperfine field as a function of temperature for various pressures (some are omitted for the sake of clarity). A reduction in the low-temperature magnetic hyperfine field was observed.

hyperfine field is continuously reduced to zero at 7.5 GPa. For this pressure, an Fe-As distance of ~ 2.37 Å can be extrapolated from reported room-temperature data [27].

It was shown that the Fe magnetic moment and thus the magnetic hyperfine field are related to the Fe-As distance which controls the Fe 3d-As 4p hybridization strength [28]. If the hybridization is strong enough, the Fe magnetic moment is quenched [29,30]. Therefore the continuous reduction of the magnetic hyperfine field to zero with decreasing Fe-As distance supports the picture that the dp hybridization strength controls the value of the iron magnetic moment. Theoretical calculations suggested that the critical Fe-As distance where the Fe magnetic moment vanishes is 2.36 Å [28]. In our paper, the critical Fe-As distance is estimated to be ~ 2.37 Å by extrapolating published data [27] which is in good agreement with the calculations. Additionally, our results are in qualitative agreement with density functional theory calculations where a reduction of the magnetic moment with increasing pressure was found [31].

Extrapolating the obtained pressure dependence of the magnetic hyperfine field to zero-pressure results in 3.7(1) T which is 1.3–1.6 T smaller than for LaFeAsO polycrystalline samples [6,18,19]. Additionally, the magnetic phase-transition temperature T_N determined by electrical

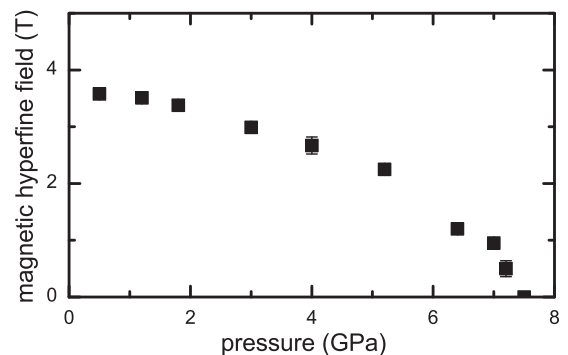


FIG. 5. Low-temperature magnetic hyperfine field for all investigated pressures. The magnetic hyperfine field is continuously reduced to zero at 7.5 GPa.

TABLE I. Low-temperature magnetic hyperfine field B for LaFeAsO as well as the magnetic phase-transition temperatures T_N at ambient pressure (if not stated otherwise).

B/T	T_N/K	
3.7(1)	127	Single crystal [7]
4.86(5)	138	Polycrystal [18]
5.1	139	Polycrystal [34]
5.19(1)	153	Polycrystal [19]
5.3	145(5)	Polycrystal, 0.1 MPa [9]
5.5		Polycrystal, 4 GPa [8]

resistivity, magnetic susceptibility, and specific-heat measurements on single crystals [7,10,32,33] has values between 117 and 127 K which are up to 36 K smaller than in polycrystalline samples [9,18,19]. Both T_N and the low-temperature magnetic hyperfine field B for single and polycrystalline samples are summarized in Table I.

Samples with smaller T_N also show a smaller B . This can be qualitatively understood in the framework of Landau theory where the magnetic order parameter M is proportional to T_N with $M \propto \sqrt{T_N}$. Therefore a reduction of T_N results in a reduction of M and thus of B .

Additionally, different samples not only deviate in T_N and B , but also deviate in the crystallographic parameters. This is shown in Fig. 6. The crystallographic a axis varies between 4.0367 [32] and 4.0308 Å [34] and thus is changed by $<0.15\%$. In contrast, the crystallographic c axis varies between 8.793 [32] and 8.7364 Å [36] and thus is changed by up to 0.65%. By increasing the unit-cell volume and, in particular, the crystallographic c axis, both T_N and B decrease. Theoretical calculations suggest that the interlayer coupling is weak but important to stabilize the magnetic order [38–40]. By increasing the crystallographic c axis and thus the interlayer distance, the interlayer coupling may decrease resulting in a weakened magnetic order. This theoretical picture is supported by the reduction of T_N and B with increasing c . However, the origin of the discrepancy in the crystallographic parameters among different samples is unknown.

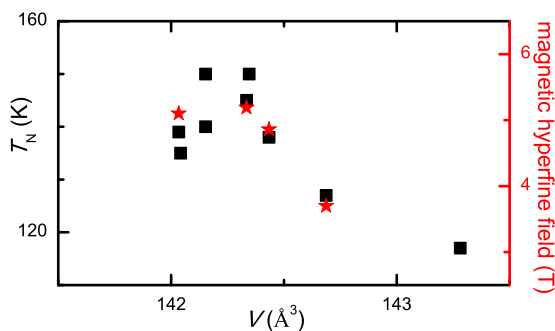


FIG. 6. T_N (black square) and low-temperature magnetic hyperfine field B (red star) as a function of the room-temperature unit-cell volume V . Unit-cell volumes and other published magnetic hyperfine fields are taken from Refs. [2,7,19,32–37]. By increasing the unit-cell volume, both T_N and B decrease.

Resistivity measurements on polycrystalline samples show a linear reduction of the magnetic phase-transition temperature between 0 and 2 GPa followed by an upturn [35]. In contrast, resistivity measurements on a single crystal show a linear reduction of T_N to 60 K at 6 GPa [10]. Energy-domain Mössbauer spectroscopy measurements of polycrystalline samples under pressure have shown 100% magnetic volume fractions at 8 GPa and 8 K [9]. At pressures of >8 GPa the magnetic volume fraction decreases with increasing pressure until a pure paramagnetic signal is observed at 24 GPa and 8 K [9]. The pressure dependence of the reported magnetic hyperfine field follows the pressure dependence of the magnetic phase-transition temperature determined by resistivity measurements in polycrystalline samples [9,35]. It shows a linear reduction between 0 and ~ 2 GPa followed by a plateau up to ~ 20 GPa and a subsequent reduction to zero [9]. In contrast, the magnetic hyperfine field obtained from SMS data on a single crystal shows a continuous reduction to zero at 7.5 GPa. The combination of the resistivity and Mössbauer experiments indicate that the single- and polycrystalline samples behave qualitatively similar at pressures below 2 GPa but differ at higher pressures.

The large difference between single crystals and polycrystals of LaFeAsO may be due to the granular and inhomogeneous natures and O deficiency at the grain boundaries of the latter. It was pointed out by McElroy *et al.* [10] that in polycrystalline samples the reduction in the resistivity at lower temperatures is very broad and it goes to zero only at 12 GPa [35] which is maybe caused by tiny amounts of O-deficient sample volumes. Mössbauer measurements by Nowik *et al.* on O-deficient LaFeAsO have shown that Fe in the vicinity of an O vacancy has a small magnetic hyperfine field of ~ 0.8 T but a huge quadrupole splitting of ~ -0.86 mm/s at low temperatures [41]. In the Mössbauer experiments under pressure of the polycrystalline samples, no O deficiency was detected. Taking into account the volume resolution of the method ($\sim 1\%$), it is in agreement with possible tiny amounts of O vacancies causing filamentary superconductivity [9,10]. Additionally, the magnetic hyperfine field of ~ 0.8 T is too small to account for the observed plateau at ~ 3 T, and therefore a significant O deficiency can be ruled out [9].

Another possible explanation are As vacancies in the polycrystalline samples. It was shown in LaFeAs $_{1-x}$ O $_{0.9}$ F $_{0.1}$ that As vacancies act as magnetic defects with a magnetic moment of $0.8\mu_B/\text{Fe}$ due to a spin polarization of the Fe 3d electrons if the Fe 3d-As 4p hybridization is sufficiently strong enough [42]. This might lead to the situation that with increasing pressure the Fe 3d-As 4p hybridization will reduce the magnetic moment but the As vacancies will enhance the spin polarization of the Fe 3d electrons and thus stabilize the magnetic order. To support or falsify this possibility, further investigations are needed.

IV. SUMMARY AND CONCLUSION

To summarize, we conducted synchrotron Mössbauer experiments at pressures up to 7.5 GPa and at temperatures between 13 and 125 K and provide a microscopic phase diagram of LaFeAsO single crystals under pressure. At the magnetic phase transition, an increase in the quadrupole splitting was

observed which is most likely of magnetic origin [20]. The magnetic hyperfine field is continuously suppressed to zero at ~ 7.5 GPa which corresponds to an Fe-As distance of ~ 2.37 Å. Our results indicate that single- and polycrystalline samples behave qualitatively similar up to 2 GPa but differ at higher pressures. A possible cause in polycrystalline samples could be due to their granular and inhomogeneous natures and O deficiency at the grain boundaries. Another possibility in polycrystalline samples could be As vacancies acting as magnetic centers as shown in Ref. [42]. We found that among different samples the magnetic phase-transition temperature as well as the low-temperature magnetic hyperfine field decrease with increasing unit-cell volume which might explain the difference in the observed quantities. Interestingly the behaviors of both LaFeAsO single crystals [10,32,33,43,44]

and polycrystalline samples [8,9,18,35] are consistent within each other.

ACKNOWLEDGMENTS

Part of this work was funded by the Deutsche Forschungsgemeinschaft (DFG, German Research Foundation) Grants No. MA 7362/1-1, No. WU 595/3-3, and No. BU 887/15-1 and the research training group GRK-1621. This research used resources of the Advanced Photon Source, a U.S. Department of Energy (DOE) Office of Science User Facility operated for the DOE Office of Science by Argonne National Laboratory under Contract No. DE-AC02-06CH11357. Support from COMPRES under NSF Cooperative Agreement No. EAR-1606856 is acknowledged for partial support of W.B.

-
- [1] Y. Kamihara, T. Watanabe, M. Hirano, and H. Hosono, *J. Am. Chem. Soc.* **130**, 3296 (2008).
- [2] H. Luetkens, H.-H. Klauss, M. Kraken, F. J. Litterst, T. Dellmann, R. Klingeler, C. Hess, R. Khasanov, A. Amato, C. Baines, M. Kosmala, O. J. Schumann, M. Braden, J. Hamann-Borrero, N. Leps, A. Kondrat, G. Behr, J. Werner, and B. Büchner, *Nat. Mater.* **8**, 305 (2009).
- [3] K. T. Lai, A. Takemori, S. Miyasaka, F. Engetsu, H. Mukuda, and S. Tajima, *Phys. Rev. B* **90**, 064504 (2014).
- [4] H. Maeter, H. Luetkens, Y. G. Pashkevich, A. Kwadrin, R. Khasanov, A. Amato, A. A. Gusev, K. V. Lamonova, D. A. Chervinskii, R. Klingeler, C. Hess, G. Behr, B. Büchner, and H.-H. Klauss, *Phys. Rev. B* **80**, 094524 (2009).
- [5] L. Pourovskii, V. Vildosola, S. Biermann, and A. Georges, *Europhys. Lett.* **84**, 37006 (2008).
- [6] M. A. McGuire, R. P. Hermann, A. S. Sefat, B. C. Sales, R. Jin, D. Mandrus, F. Grandjean, and G. J. Long, *New J. Phys.* **11**, 025011 (2009).
- [7] R. Kappenberger, S. Aswartham, F. Scaravaggi, C. G. Blum, M. I. Sturza, A. U. Wolter, S. Wurmehl, and B. Büchner, *J. Cryst. Growth* **483**, 9 (2018).
- [8] R. S. Kumar, J. J. Hamlin, M. B. Maple, Y. Zhang, C. Chen, J. Baker, A. L. Cornelius, Y. Zhao, Y. Xiao, S. Sinogeikin, and P. Chow, *Appl. Phys. Lett.* **105**, 251902 (2014).
- [9] T. Kawakami, T. Kamatani, H. Okada, H. Takahashi, S. Nasu, Y. Kamihara, M. Hirano, and H. Hosono, *J. Phys. Soc. Jpn.* **78**, 123703 (2009).
- [10] C. A. McElroy, J. J. Hamlin, B. D. White, S. T. Weir, Y. K. Vohra, and M. B. Maple, *Phys. Rev. B* **90**, 125134 (2014).
- [11] W. Bi, J. Zhao, J.-F. Lin, Q. Jia, M. Y. Hu, C. Jin, R. Ferry, W. Yang, V. Struzhkin, and E. E. Alp, *J. Synchrotron Radiat.* **22**, 760 (2015).
- [12] J. Y. Zhao, W. Bi, S. Sinogeikin, M. Y. Hu, E. E. Alp, X. C. Wang, C. Q. Jin, and J. F. Lin, *Rev. Sci. Instrum.* **88**, 125109 (2017).
- [13] W. Sturhahn, *Hyperfine Interact.* **125**, 149 (2000).
- [14] W. Sturhahn, E. Alp, T. Toellner, P. Hession, M. Hu, and J. Sutter, *Hyperfine Interact.* **113**, 47 (1998).
- [15] W. Sturhahn, *J. Phys.: Condens. Matter* **16**, S497 (2004).
- [16] I. Sergueev, R. P. Hermann, D. Bessas, U. Pelzer, M. Angst, W. Schweika, M. A. McGuire, A. S. Sefat, B. C. Sales, D. Mandrus, and R. Rüffer, *Phys. Rev. B* **87**, 064302 (2013).
- [17] F. J. Lynch, R. E. Holland, and M. Hamermesh, *Phys. Rev.* **120**, 513 (1960).
- [18] H.-H. Klauss, H. Luetkens, R. Klingeler, C. Hess, F. J. Litterst, M. Kraken, M. M. Korshunov, I. Eremin, S.-L. Drechsler, R. Khasanov, A. Amato, J. Hamann-Borrero, N. Leps, A. Kondrat, G. Behr, J. Werner, and B. Büchner, *Phys. Rev. Lett.* **101**, 077005 (2008).
- [19] M. A. McGuire, A. D. Christianson, A. S. Sefat, B. C. Sales, M. D. Lumsden, R. Jin, E. A. Payzant, D. Mandrus, Y. Luan, V. Keppens, V. Varadarajan, J. W. Brill, R. P. Hermann, M. T. Sougrati, F. Grandjean, and G. J. Long, *Phys. Rev. B* **78**, 094517 (2008).
- [20] P. Materne, W. Bi, E. E. Alp, J. Zhao, M. Y. Hu, A. Jesche, C. Geibel, R. Kappenberger, S. Aswartham, S. Wurmehl, B. Büchner, D. Zhang, T. Goltz, J. Spehling, and H.-H. Klauss, *Phys. Rev. B* **98**, 014517 (2018).
- [21] A. Błachowski, K. Ruebenbauer, J. Zukrowski, J. Przewoznik, K. Wojciechowski, and Z. Stadnik, *J. Alloys Compd.* **494**, 1 (2010).
- [22] R. D. Renzi, P. Bonfà, M. Mazzani, S. Sanna, G. Prando, P. Carretta, R. Khasanov, A. Amato, H. Luetkens, M. Bendele, F. Bernardini, S. Massidda, A. Palenzona, M. Tropeano, and M. Vignolo, *Supercond. Sci. Technol.* **25**, 084009 (2012).
- [23] P. Materne, S. Kamusella, R. Sarkar, T. Goltz, J. Spehling, H. Maeter, L. Harnagea, S. Wurmehl, B. Büchner, H. Luetkens, C. Timm, and H.-H. Klauss, *Phys. Rev. B* **92**, 134511 (2015).
- [24] T. Goltz, V. Zinth, D. Johrendt, H. Rosner, G. Pascua, H. Luetkens, P. Materne, and H.-H. Klauss, *Phys. Rev. B* **89**, 144511 (2014).
- [25] G. Prando, O. Vakaliuk, S. Sanna, G. Lamura, T. Shiroka, P. Bonfà, P. Carretta, R. De Renzi, H.-H. Klauss, C. G. F. Blum, S. Wurmehl, C. Hess, and B. Büchner, *Phys. Rev. B* **87**, 174519 (2013).
- [26] A. Ricci, N. Poccia, B. Joseph, L. Barba, G. Arrighetti, G. Ciasca, J.-Q. Yan, R. W. McCallum, T. A. Lograsso, N. D. Zhigadlo, J. Karpinski, and A. Bianconi, *Phys. Rev. B* **82**, 144507 (2010).
- [27] K. Kobayashi, J.-i. Yamaura, S. Iimura, S. Maki, H. Sagayama, R. Kumai, Y. Murakami, H. Takahashi, S. Matsuishi, and H. Hosono, *Sci. Rep.* **6**, 39646 (2016).
- [28] S. Mirbt, B. Sanyal, C. Isheden, and B. Johansson, *Phys. Rev. B* **67**, 155421 (2003).

- [29] T. M. McQueen, M. Regulacio, A. J. Williams, Q. Huang, J. W. Lynn, Y. S. Hor, D. V. West, M. A. Green, and R. J. Cava, *Phys. Rev. B* **78**, 024521 (2008).
- [30] J. Wu, P. Phillips, and A. H. Castro Neto, *Phys. Rev. Lett.* **101**, 126401 (2008).
- [31] I. Opahle, H. C. Kandpal, Y. Zhang, C. Gros, and R. Valentí, *Phys. Rev. B* **79**, 024509 (2009).
- [32] C. A. McElroy, J. J. Hamlin, B. D. White, M. A. McGuire, B. C. Sales, and M. B. Maple, *Phys. Rev. B* **88**, 134513 (2013).
- [33] A. Jesche, F. Nitsche, S. Probst, T. Doert, P. Müller, and M. Ruck, *Phys. Rev. B* **86**, 134511 (2012).
- [34] H. Raffius, E. Mörsen, B. Mosel, W. Müller-Warmuth, W. Jeitschko, L. Terbüchte, and T. Vomhof, *J. Phys. Chem. Solids* **54**, 135 (1993).
- [35] H. Okada, K. Igawa, H. Takahashi, Y. Kamihara, M. Hirano, H. Hosono, K. Matsubayashi, and Y. Uwatoko, *J. Phys. Soc. Jpn.* **77**, 113712 (2008).
- [36] N. Qureshi, Y. Drees, J. Werner, S. Wurmehl, C. Hess, R. Klingeler, B. Büchner, M. T. Fernández-Díaz, and M. Braden, *Phys. Rev. B* **82**, 184521 (2010).
- [37] T. Nomura, S. W. Kim, Y. Kamihara, M. Hirano, P. V. Sushko, K. Kato, M. Takata, A. L. Shluger, and H. Hosono, *Supercond. Sci. Technol.* **21**, 125028 (2008).
- [38] O. Andersen and L. Boeri, *Ann. Phys.* **523**, 8 (2011).
- [39] C. Xu, M. Müller, and S. Sachdev, *Phys. Rev. B* **78**, 020501 (2008).
- [40] S.-P. Kou, T. Li, and Z.-Y. Weng, *Europhys. Lett.* **88**, 17010 (2009).
- [41] I. Nowik, I. Felner, V. P. S. Awana, A. Vajpayee, and H. Kishan, *J. Phys.: Condens. Matter* **20**, 292201 (2008).
- [42] V. Grinenko, K. Kikoin, S.-L. Drechsler, G. Fuchs, K. Nenkov, S. Wurmehl, F. Hammerath, G. Lang, H.-J. Grafe, B. Holzapfel, J. van den Brink, B. Büchner, and L. Schultz, *Phys. Rev. B* **84**, 134516 (2011).
- [43] M. Fu, D. A. Torchetti, T. Imai, F. L. Ning, J.-Q. Yan, and A. S. Sefat, *Phys. Rev. Lett.* **109**, 247001 (2012).
- [44] J. M. Ok, S.-H. Baek, D. V. Efremov, R. Kappenberger, S. Aswartham, J. S. Kim, J. van den Brink, and B. Büchner, *Phys. Rev. B* **97**, 180405 (2018).